NIPPON STEEL TECHNICAL REPORT No. 102 JANUARY 2013

Technical Report

UDC 539 . 4 . 072 : 620 . 186

Model for the Prediction of Microstructures and Mechanical Properties of Cold-rolled High Strength Steels

Masafumi AZUMA* Manabu TAKAHASHI
Nobuhiro FUJITA

Abstract

Microstructure development of advanced high strength steels is quiet complicated and, thereby, it takes much time to develop advanced high strength steels. This paper presents a complete model which can simulate microstructure development of high strength steels during a heat treatment and the mechanical properties after the treatment. The model consisting of ferrite, bainite, martensite and predicting stress-strain curve of the steels is successively built based on metallurgical phenomena.

1. Introduction

The requirements for improvement of the fuel efficiency of automobiles and the reduction of their CO_2 emissions are growing more extensive from the viewpoint of conservation of the global environment. On the other hand, the higher strength of car bodies is indispensable for protecting passengers. The use of higher strength steel sheets for car bodies is thus effective for reducing the weight of automobiles while improving their strength. A higher strength for steel sheets, however, leads to reduced ductility (poorer uniform elongation), and for this reason, it is necessary to improve both the strength and the formability of steel sheets simultaneously. As a response, Nippon Steel Corporation developed dual phase (DP) steels with a metallographic structure of ferrite and martensite, and transformation-induced plasticity (TRIP) steels consisting of ferrite, bainite, and retained austenite (γR), and launched sheet products made of these steels into the market for the first time in the world.[1-4] The DP steel sheets ensure high ductility due to the use of the soft ferrite, while still maintaining high strength because of the dispersion of hard martensite in the matrix. In contrast, the TRIP steel sheets exhibit excellent uniform elongation due to the transformation-induced plasticity of the retained austenite dispersed in the matrix.[3, 4]

To manufacture the sheets of these steels, however, it is necessary to control two or more phase transformations simultaneously, and the effects of the alloying elements and heat treatment conditions on the microstructure are widely varied. For this reason, development of such new products requires a variety of repeated experiments involving a great deal of cost and time. In consideration of this issue, there have been attempts to predict the microstructure and material quality of steel sheets through numerical operations as an alternative to the use of conventional experimental approaches. In order to predict the characteristics of high-strength steel sheets, however, it is necessary to address the very complicated interrelationships of two or more competitive phase transformation reactions. In addition, there are no calculation models capable of simulating the formation of the bainite transformation accompanying cementite deposition, or any that can predict the stress-strain curves of multiphase steel sheets. Given this situation, Nippon Steel Corporation, jointly with Arcelor (now Arcelor Mittal), embarked upon the development of a quality prediction model that could predict in a comprehensive manner all of the aspects of steel sheet formation, from microstructural development during heat treatment to the product stress-strain curves. This paper outlines the development of this model.

2. Prediction of Microstructural Development during Manufacturing Processes and Stress-Strain Curves of Steel During Plastic Deformation

The production processes for DP and TRIP steel sheets include hot- and cold-rolling followed by either continuous annealing or continuous hot-dip galvanizing, and are typical of steel sheet products. Hot-rolled coils are cooled to room temperature, for example, sometimes over a period of several days, while continuous annealing takes

* Senior Researcher, Sheet Products Lab., Steel Research Laboratories
20-1, Shintomi, Futtsu, Chiba 293-8511

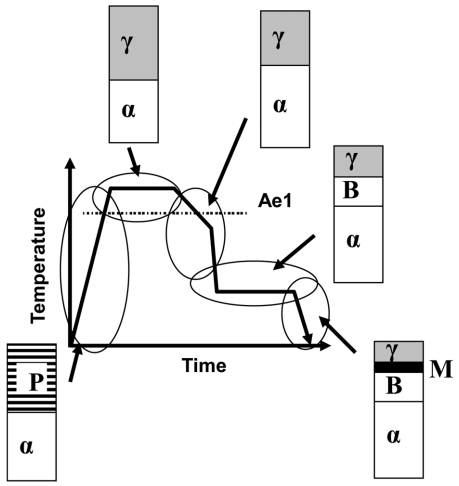

Fig. 1 Schematic illustration of phase transformation behavior during continuous annealing processing line
α : Ferrite, P : Pearlite, B : bainite, M : martensite, γ : austenite

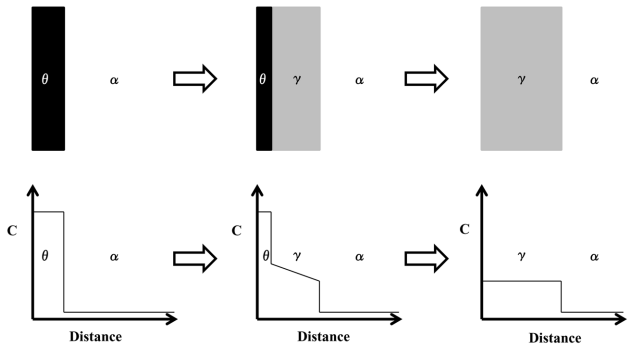

Fig. 2 Reverse transformation from cementite to austenite during intercritical annealing

only tens of minutes. When the same material quality is desired with different steels that undergo heat treatment through different production facilities, the steels must be of different chemistries suitable for the respective heat treatment conditions. However, given the very wide variety of combinations of steel chemistries and manufacturing conditions available for defining the best steel chemistry and production route for a desired material quality, it is necessary to repeatedly conduct numerous different tests, which takes a significant amount of time. To solve this problem, development of a comprehensive quality prediction model capable of dealing with DP and TRIP steels, and covering the manufacturing process from microstructural development to generation of the stress-strain curves of the final product, was initiated.

First, an example is used to help explain what was envisaged for the prediction model. **Fig. 1** schematically shows the microstructural changes in hot- and cold-rolled steel sheets during continuous annealing. A microstructure prediction model can deal with two or more phase transformations that take place during a heat treatment process, namely (1) reverse transformation from hot-rolled steel sheets, and (2) ferrite, (3) bainite, and (4) martensite transformations during cooling. The intention in the development of the quality prediction model was to obtain, in addition, the stress-strain curves of the product using the estimated metallographic parameters, such as the volume fraction, grain size, etc., for the resulting metallographic phases.

2.1 Reverse transformation for hot-rolled steel sheet

In order to minimize the load during cold rolling, the microstructure of hot-rolled sheets used as the material for manufacturing high-strength, cold-rolled or galvannealed sheets is often made so as to consist of ferrite (α) and pearlite. When these sheets are cold-rolled and annealed to the two-phase temperature range of ferrite and austenite (γ), cementite (θ) in the steel transforms into austenite[5-7]; this reaction, shown in **Fig. 2**, is called reverse transformation. The reaction that takes place here can be expressed by Equation (1), which is called the Johnson-Mehl-Avrami equation:

$$f^{\gamma} = f_{eq}(1 - \exp(-bt^{n})) \quad (1)$$

$$df^{\gamma} = f^{\gamma}_{eq}(bnt^{n-1}) \exp(-bt^{n})\, dt \quad (2)$$

where f^{γ} is the volume fraction of γ, f^{γ}_{eq} is the same in the paraequilibrium at different temperatures above Ac_1, b is a fitting parameter, t is the transformation time (holding time), and n is the Avrami factor. Andrew's equation given below was used for calculating the starting temperature of the reverse transformation, Ac_1[8]:

$$Ac_1\,[^{\circ}C] = 723 - 10.7Mn + 29.1Si + 16.9Cr \quad (3)$$

2.2 Ferritic transformation during cooling

The microstructure obtained through annealing in the two-phase range consists of ferrite and austenite. Because ferrite generally exists in great quantities after annealing in this temperature range, it was assumed that ferritic transformation would advance during cooling due to the growth of the ferrite. In addition, assuming that a local equilibrium is established at the ferrite/austenite boundaries during ferrite growth, the growth of the ferrite in both the partitioning local equilibrium (PLE) mode (where the ferrite growth rate is governed by the diffusion of substitutional elements) and the negligible partitioning local equilibrium (NPLE) mode (where the ferrite growth rate is governed by the diffusion of carbon) was incorporated in the prediction model. Meanwhile, some researchers have pointed out that energy is wasted as elements that have segregated at the phase boundaries are dragged by the shift of the boundaries.[9] In the present model, the mobility (v) of the ferrite/austenite boundaries was defined according to the methods proposed by Krielaart, Zwaag, Hillert, et al. as follows [10, 11]:

$$v = M\Delta\mu_{Fe} \quad (4)$$

where $\Delta\mu_{Fe}$ is the differential chemical potential between ferrite and austenite, and M is the mobility of the ferrite/austenite boundaries, which is given as a function of the temperature.[9]

2.3 Bainitic transformation with cementite precipitation

Bainitic transformation begins when steel is cooled to below Bs, the bainitic transformation starting temperature. The microstructure of bainite is known to appear as upper bainite containing cementite between bainite laths, or lower bainite containing cementite inside the laths, depending on the transformation temperature (see **Fig. 3**).[12] When upper bainite appears, austenite exists between the laths before the cementite precipitates, and when the cementite precipitates, the austenite disintegrates into the bainitic laths and cementite. Bhadeshia et al. maintain that a bainitic lath is composed of fine particles, called sub-units, which form by a displacive transformation mechanism similar to that by which martensite forms.

In the present model, the formation of the sub-units was also regarded as resulting from the displacive transformation mechanism following the method of Bhadeshia et al.[13] On the other hand, lath martensite and its sub-units are known to form through an autocatalytic mechanism.[14] For this reason, it was also assumed in the present

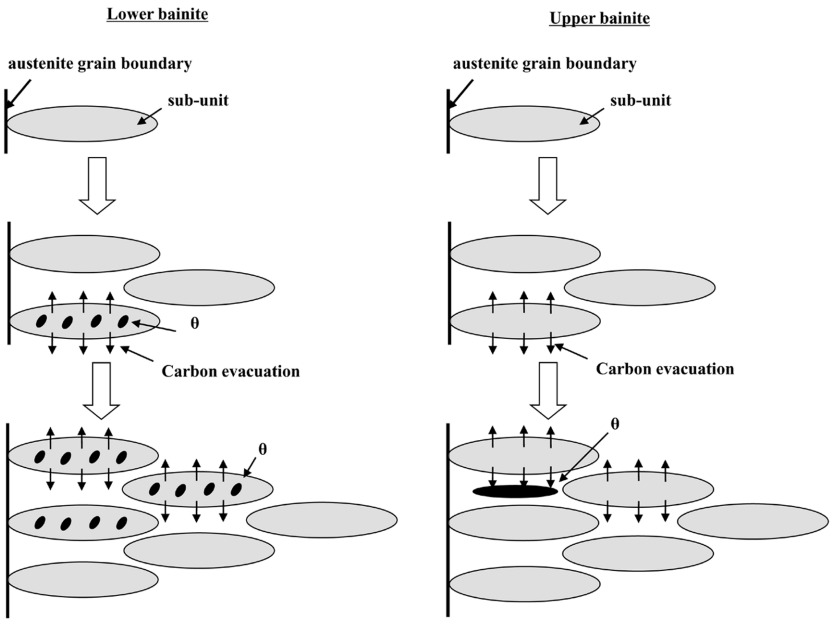

Fig. 3 Schematic illustration of upper bainite and lower bainite transformation

model that the sub-units comprising the bainitic structure formed as a result of the autocatalytic mechanism, and the number of their nucleation sites could be expressed as a function of the volume fraction of bainitic ferrite. The size of the sub-units, on the other hand, is known to depend on the hardness of the austenite parent phase and the driving force of its transformation.[15] Based on this behavior, in the developed model, the size of the sub-units is expressed as a function of the hardness and the transformation driving force of the austenite, and the volume fraction of the bainite is assumed to increase as the sub-units form autocatalytically. Bainitic ferrite forming through the displacive transformation mechanism contains supersaturated carbon, but because it is unstable in bainitic ferrite, it diffuses into the surrounding austenite or precipitates within the bainitic ferrite as cementite. Because the rate of carbon diffusion in austenite is low, it was assumed that the rate of carbon diffusion from the bainitic ferrite into the austenite depends on its diffusion rate in austenite, and the carbon concentration in the bainitic ferrite is influenced by the mass balance of the carbon between the austenite and bainitic ferrite. On the other hand, there have been reports that the cementite in upper or lower bainite precipitates under para-equilibrium conditions when there is no diffusion of substitutional elements. Based on these results, cementite precipitation under para-equilibrium conditions was included in the model.[16] The thermodynamic parameters necessary for the phase transformation calculations were obtained using the Thermo-Calc software.

When the driving force for cementite precipitation is sufficiently strong, cementite precipitates inside the bainite laths before carbon diffuses into the austenite. Therefore, it was assumed that, particularly when the temperature is low, and consequently, carbon diffusion is slow and the driving force for cementite precipitation is strong, lower bainite would result, wherein the cementite precipitates inside the bainite laths.

In summary, the following four competitive reactions were included in the developed model: (1) formation of bainitic ferrite by the displacive transformation mechanism; (2) diffusion of supersaturated carbon in the bainitic ferrite into the austenite; (3) precipitation of cementite in the austenite; and (4) precipitation of cementite in the bainitic ferrite.

2.4 Martensitic transformation

Martensitic transformation takes place when a steel containing austenite is cooled to below the martensite starting temperature, at which point the austenite begins to transform into martensite (the Ms temperature). It has been empirically known that the volume fraction of athermally transformed martensite is given as a function of the supercooling below the Ms temperature.[17] Based on this knowledge, the volume fraction of martensite (f^M) during or after cooling was estimated using the following equation:

$$f^M = f^\gamma \, (1 - 0.011\exp(Ms - T)) \quad (5)$$

where f^γ is the volume fraction of γ, and T is the cooling end temperature.

2.5 Prediction of stress-strain curves

High-strength steel sheets, such as those of DP and TRIP steels, are composed of two or more constituents with different properties, and partitioning of the strain and stress is different between the phases, which makes the prediction of product properties complicated. Although there are models capable of predicting the stress-strain curves of individual phases, there are few capable of predicting them for DP, TRIP, and similar steels with complicated microstructures. Given this situation, a model that could predict the properties of steel sheets with a multi-phase structure was envisaged.

In order to predict the properties of high-strength steel sheets containing retained austenite, it is necessary to take into consideration: i) the stress-strain curves of the component phases; ii) the stress/strain partitioning between the phases; and iii) the martensitic transformation during deformation. In particular, when predicting the properties of sheets of TRIP steels, the uniform elongation of which is increased by making use of the transformation-induced plasticity of the retained austenite, consideration of the martensitic transformation during deformation is indispensable. The formulae for the stress-strain curves of constituents were obtained by:

- experimentally determining the stress-strain curves of single-phase structure specimens of different chemistries prepared

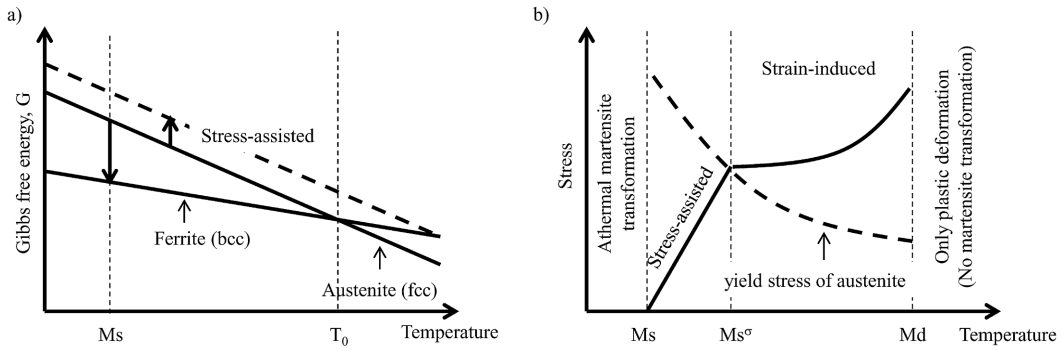

Fig. 4 Relationship between stress-assisted and strain-induced martensite

under different heat treatment conditions;

- investigating the influence of the different strengthening mechanisms over the stress-strain curve; and
- defining the effects of grain size, precipitates, and solid solution hardening throughout the stress-strain relationships of the different phases.

Subsequently, it was necessary to obtain the stress-strain curves of steel sheets with multi-phase structures from that of each component phase.

In general, hard martensite and bainite are more resistant to deformation than soft ferrite, and consequently, when work is applied to a composite-phase steel with a main ferrite phase combined with a hard phase or hard phases, the stress and strain are partitioned between the main and the hard phases.[18-23] For this reason, it is impossible to reproduce the stress-strain curve of steel sheets of a multi-phase structure applying a simple rule of mixtures, such as the equal-stress or equal-strain hypothesis. The finite element method (FEM)[24], the secant method [25, 26], and the Iso-Work method [27, 28], etc,. were therefore proposed as possible methods for solving this problem and predicting the stress and strain partitioning within steel sheets having a multi-phase structure.

FEM analysis is a method for obtaining the stress-strain relationship within a material as a continuum from the stress-strain relationships of various component phases based on continuum mechanics. While FEM analysis is capable of defining the local strain distribution within a microstructure, the calculation takes a long time and is considerably costly. Therefore, it is unsuitable for predicting the influence of alloying elements and heat treatment conditions for all of the product properties in a simple manner. Using the secant method, on the other hand, it is possible to obtain the stress partitioning between a main phase and a hard phase under different strains by considering the hard phase as a virtual elastic body. This method can provide a rather simple stress partitioning between the soft and the hard phases of a dual-phase steel, but its application is very complicated when dealing with steels consisting of three or more phases in which the transformation-induced plasticity of retained austenite is involved.

In contrast, with the Iso-Work method, the partitioning of strain between the constituents is obtained assuming that the work of a component phase is equal to that of another; therefore, it can deal with the strain partitioning between phases in a comparatively simple and easy manner. Thus, the Iso-Work method was applied for defining the stress and strain partitioning between phases.

When plastic work is applied to a steel sheet containing retained austenite (γR), it transforms into martensite, leading to an increase in work hardening and an improvement in the uniform elongation.[3, 4] In order to predict the properties of steel sheets, and particularly of TRIP steel sheets, that use retained austenite to improve the uniform elongation, modeling of the transformation-induced plasticity is absolutely essential. The strengthening effect by stress-assisted and strain-induced transformation is known to depend on the volume fraction of martensite, the transformation product.

In view of the above, the stress-assisted and strain-induced martensitic transformations during deformation were modeled. During continuous cooling, martensite forms at nucleation sites in austenite at temperatures below the Ms temperature. As can be seen in **Fig. 4**, when a stress is applied, the driving force for the martensitic transformation at those sites is partially borne by the stress, and the martensitic transformation takes place as a result. Given this behavior, the stress-assisted martensitic transformation was incorporated into the developed model. In addition, the strain resulting from plastic deformation also accelerates the martensitic transformation. Olson, Choen, Raghavan, and others formulated this strain-induced martensitic transformation into models.[29, 30] A similar modeling method was therefore employed in order to incorporate the martensitic transformation during deformation into the developed model.

Fig. 5 schematically shows the procedures for calculating the stress-strain relationship using the Iso-Work method. For simplicity's

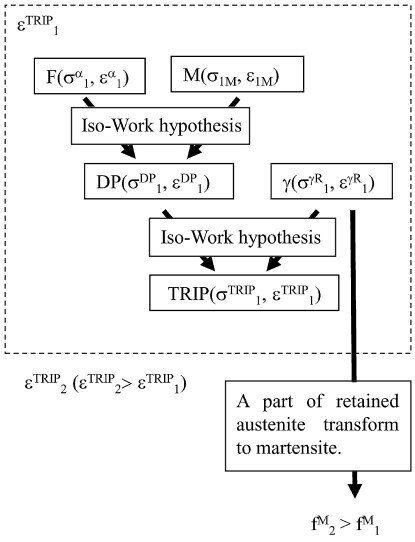

Fig. 5 Schematic illustration of flow chart to calculate mechanical properties of TRIP steel

sake, this example shows the calculation steps for a microstructure consisting of ferrite, martensite, and retained austenite. Based on the Iso-Work method, the following equations were assumed to hold true for the stress and strain of each structural phase:

$$\sigma^{TRIP}{}_1 = f^{\alpha} \times \sigma^{\alpha}{}_1 + f^{M} \times \sigma^{M}{}_1 + f^{\gamma R} \times \sigma^{\gamma R}{}_1 \quad (6)$$

$$\varepsilon^{TRIP}{}_1 = f^{\alpha} \times \varepsilon^{\alpha}{}_1 + f^{M} \times \varepsilon^{M}{}_1 + f^{\gamma R} \times \varepsilon^{\gamma R}{}_1 \quad (7)$$

$$\int_i^{i+1} \sigma^{\alpha} d\varepsilon^{\alpha} = \int_i^{i+1} \sigma^{M} d\varepsilon^{M} = \int_i^{i+1} \sigma^{\gamma R} d\varepsilon^{\gamma R} \quad (8)$$

where σ^i_j and ε^i_j ($i = \alpha$: ferrite, M: martensite, γR: retained austenite) are the true stress and true strain, respectively, of each phase under application of a true strain of ε^{TRIP}_j ($\varepsilon^{TRIP}{}_2 > \varepsilon^{TRIP}{}_1$), and f^i is the volume fraction of each phase.

3. Comprehensive Prediction from Microstructure to Mechanical Properties

3.1 Experimental procedure

To verify the effectiveness of the developed model for comprehensively predicting the expected microstructure due to heat treatment through to the stress-strain relationship of the product, the following test was carried out. A steel containing 0.1 mass% C, 1.2 mass% Si, and 1.2 mass% Mn was vacuum melted, hot-rolled, and then cold-rolled into thin sheets. The sheets were annealed at 800˚C (in the ferrite and austenite region) for 120 s, and then held at 450˚C for 0, 100, and 300 s under the conditions shown in **Fig. 6** in order to generate different microstructures. The microstructures thus obtained were observed by optical microscopy, and the volume fraction and the C content of the retained austenite were measured by X-ray diffractometry. The tensile properties were measured using an Instron tensile machine at a crosshead speed of 10 mm/min. The experimental data were then compared with the calculated results.

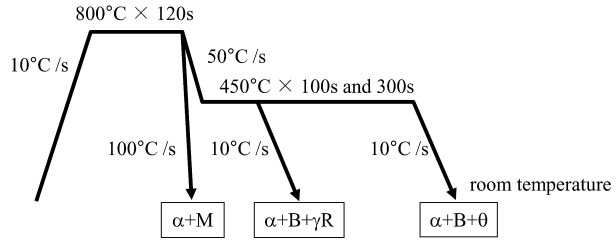

Fig. 6 Heat cycles

3.2 Comparison of experimental and calculated results

Fig. 7 shows the microstructures of the steel sheets obtained from the process described above. As seen here, the microstructures of all of the specimens consisted mainly of ferrite accompanied by hard phases of martensite, bainite, and/or retained austenite. Measurement of the volume fractions and grain sizes of the component phases revealed the following (see **Table 1**). The microstructure of the sheets that were not held at 450˚C (0 s) consisted of ferrite and martensite, corresponding to that of DP steel. Those held at 450˚C for 100 s underwent bainitic transformation during the holding, which led to carbon condensation in the austenite, and consequently, the microstructure included retained austenite. In contrast, in the sheets that were held at 450˚C for 300 s, cementite precipitated, leading to disintegration of the retained austenite, and as a result, the microstructure was composed of ferrite and bainite containing cementite. Observation at higher magnifications through a transmission electron microscope (TEM) revealed that the bainite was upper bainite with cementite between the laths of bainitic ferrite. Because cementite was included in the bainite, in the determination of the volume fractions for the developed model, this cementite was counted as part of the bainite. The specimens prepared through the above processes were found to correspond, respectively, to DP steel, TRIP steel, and steel composed of ferrite and bainite.

For verification purposes, the effects of the steel chemistry and heat treatment conditions described in Sub-section 3.1 on the metallographic parameters were estimated using the developed prediction model. As seen in Table 1 and **Fig. 8**, the estimated results agreed well with the actual measurement results in terms of the volume frac-

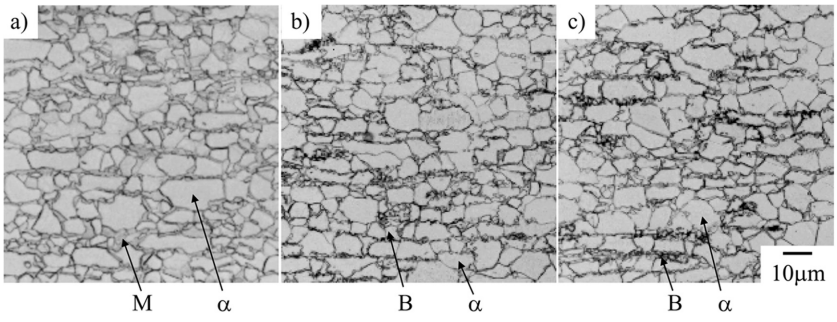

Fig. 7 Microstructure after heat treatment

a) 0s, b) 100s and c) 300s. A steel without isothermal holding consists of ferrite and martensite. A steel annealed at 450˚C for 100s contains ferrite, bainite and retained austenite and retained austenite is composed to bainite and cementite in a steel annealed for 300s.

Table 1 Experimental and calculated microstructure

	Measured volume fraction (%)				Measured	Calculated volume fraction (%)				Calculated
	f^{α}	f^{B}	$f^{\gamma R}$	f^{M}	$d\alpha$ (μm)	f^{α}	f^{B}	$f^{\gamma R}$	f^{M}	$d\alpha$ (μm)
0s	75.6	0	0.9	23.5	5.9	78.1	1.0	1.8	19.1	5.2
100s	82.3	12.3	4.3	1.1	6.1	83.8	8.4	5.6	2.2	5.8
300s	82.3	17.7	0	0	6.1	83.8	15.4	0.8	0	5.8

tions and grain sizes of the component structural phases and the C concentration in the retained austenite (an indicator of the stability of the retained austenite) under all of the heat treatment conditions. These results therefore indicate that the developed model is good for the prediction of the microstructure of multi-phase steel sheets, including high-strength DP and TRIP steels.

Additionally, the true stress-true strain curves and tensile characteristics of the specimens were calculated based on the information obtained for the predicted microstructures. **Fig. 9** shows the stress-strain curves and work hardening rates calculated for the specimens under different strains. As can be seen in the figure, the work hardening rate of the specimens not held at 450˚C (0 s) is high in the low strain range, reflecting well the characteristic behavior of DP steel. The prediction result for the specimens held 450˚C for 100 s, which contained retained austenite, reflects the characteristics of TRIP steel, namely, work hardening rates low in the low strain range, but high in the high strain range due to transformation-induced plasticity, and excellent uniform elongation. On the other hand, for the specimens held for 300 s at 450˚C, in which the retained austenite had disintegrated, both the estimated work hardening rate and flow stress were low.

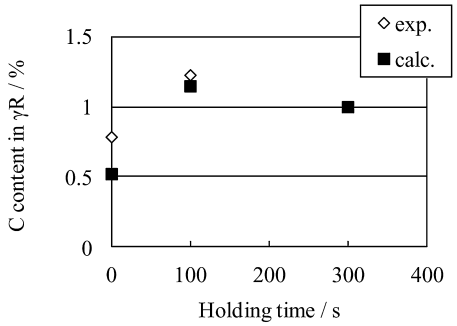

Fig. 8 Carbon (C) contents in retained austenite after heat treatment

The ultimate tensile strength and uniform elongation of the specimen sheets were then calculated based on the relationship between the true stress and true strain estimated for them. It has been known that the initiation of necking during the tensile test is closely related to the plastic instability. Therefore, the point on the true stress-true strain curve where the following condition is satisfied indicates the true stress and true strain at the start of necking:

$$d\sigma / d\varepsilon = \sigma \quad (9)$$

The ultimate tensile strength (TS) and uniform elongation (UEl) were calculated by converting these values into the nominal stress and nominal strain, respectively. As **Fig. 10** shows, the ultimate tensile strength of the specimens not held at 450˚C (0 s) was high, and the uniform elongation was small. The calculated results for the specimens held at 450˚C for 100 s, which contained retained austenite, well reproduced the characteristic, excellent uniform elongation of TRIP steel. In contrast, both the calculated ultimate tensile strength and uniform elongation for the specimens held at 450˚C for 300 s, the microstructure of which consisted of ferrite and bainite, were low.

The model predictions were in good agreement with the experimental results for all of the specimens prepared under different heat treatment conditions. These results demonstrate that the developed model is effectively applicable for predicting the properties of steel sheets of DP, TRIP, and other types of multi-phase steels.

The developed model, however, has a problem in that it cannot predict the strain at the fracture of steel sheets, such as that at the

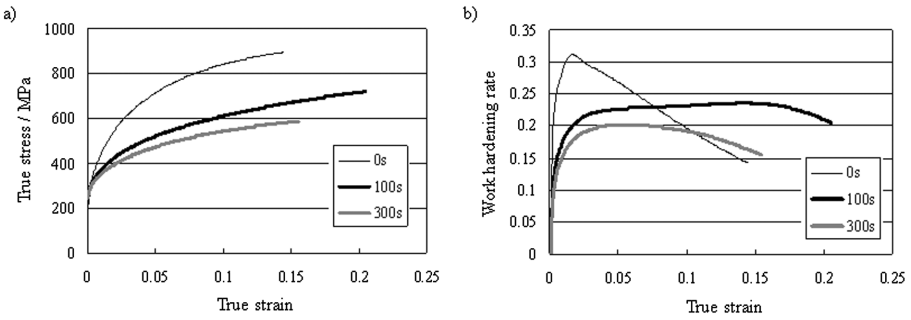

Fig. 9 Effect of heat treatment on mechanical properties
a) True stress-true strain curves, b) Work hardening rate

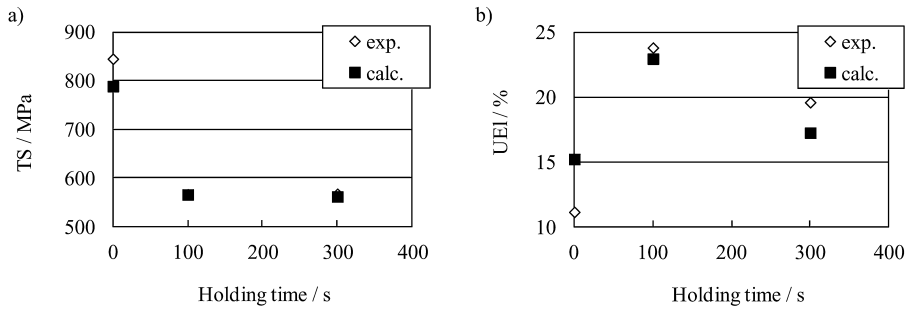

Fig. 10 Tensile properties after heat treatment
a) Ultimate tensile strength (TS), b) Uniform elongation (UEl)

measurement of total elongation. Further efforts are therefore required in order to expand the applicability of the quality prediction model to the local elongation and other properties relevant to thin sheet products.

4. Conclusions

A comprehensive material quality calculation model capable of predicting the microstructure of DP, TRIP and other multi-phase steels, as well as their stress-strain curves, has been developed. The model is expected to be instrumental in enhancing the efficiency of existing steel sheet product manufacturing and the development of new products. The rapid development of products with higher functionality is required in order to cope with quickly changing social environments. Specifically, rapid product development combined with the pursuit of extreme material properties that maximizes the advantages of computational technology is desirable for enabling more effective responses to customer requirements.

References

1) Akisue, O., Hata, R.: Shinnittetsu Giho. (354), 1 (1994)
2) Nonaka, T., Gotoh, K., Taniguchi, Y., Yamazaki, K.: Shinnittetsu Giho. (378), 12 (2003)
3) Matsumura, O., Sakuma, Y., Takechi, H.: Scripta Metallurgica. 21, 1301 (1987)
4) Sakuma, Y., Kimura, N., Itami, J., Hiwatashi, S., Kohno, O., Sakata, K.: Shinnittetsu Giho. (354), 17 (1994)
5) Roberts, G. A., Mehl, R. F.: Trans. ASM. 31, 613 (1943)
6) Judd, R. R., Paxton, H. W.: Trans. Metall. Soc.AIME. 242, 206 (1968)
7) Atkinson, C., Akbay, T., Reed, R. C.: Acta Metall. Mater. 43, 213 (1995)
8) Andrews, K. W.: J. Iron Steel Inst. 203, 721 (1965)
9) Van der Ven, A., Delaey, L.: Prog. Mater. Sci. 40, 181 (1996)
10) Krielaart, G.P., van der Zwaag, S.: Mat. Sci. Eng. A237, 216 (1997)
11) Hillert, M.: Metall. Trans. 6A, 5 (1975)
12) Bhadeshia, H. K. D. H.: Bainite in Steels. The Institute of Materials, 1992
13) Ali, A., Bhadeshia, H. K. D. H.: Mater. Sci. Tech. 6, 781 (1990)
14) Rees, G. I., Bhadeshia, H. K. D. H.: Mater. Sci. Tech. 8, 985 (1992)
15) Singh, S. B., Bhadeshia, H. K. D. H.: Mater. Sci. Eng. A245, 72 (1998)
16) Azuma, M., Fujita, N., Takahashi, M., Iung, T.: ISIJ International. 45, 221 (2005)
17) Magee, C.L.: The Nucleation of Martensite, Ch. 3. ASM, New York, 1968
18) Morooka, S., Tomota, Y., Kamiyama, T.: ISIJ International. 48, 525 (2008)
19) Asoo, K., Tomota, Y., Harjo, S., Okitsu, Y.: ISIJ International. 51, 145 (2011)
20) Su, Y. L., Gurland, J.: Mat. Sci. Eng.. 95, 151 (1987)
21) Osokov, Y., Wilkinson, D. S., Jain, M., Simpson, T.: Int. J. Mater. Res. 98, 664 (2007)
22) Kang, J., Ososkov, Y., Embury, J. D., Wilkinson, D. S.: Scripta Mater. 56, 999 (2007)
23) Azuma, M., Hansen, N., Winther, G., Stequio, G., Huang, X.: Mater. Sci. Tech. In press.
24) Sun, X., Choi, K.S., Soulami, A., Liu, W.N., Khaleel, M.A.: Mater. Sci. Eng. A 526, 140 (2009)
25) Weng, G.J.: J. Mech. Phys. Solid. 38, 419 (1990)
26) Koyama, T.: Tetsu-to-Hagané. 97, 212 (2011)
27) Bouaziz, O., Buessler, P.: Revue de Metallurgie. 1, 71 (2002)
28) Olson, G. B., Choen, M.: Metall. Trans. 6A, 791 (1975)
29) Olson, G. B., Choen, M.: Metall. Trans. 7, 1897 (1976)
30) Raghavan, V., Entwisle, A. R.: J. Iron Steel Inst. 93, 110 (1965)

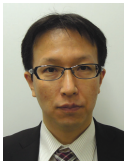

Masafumi AZUMA
Senior Researcher
Sheet Products Lab.
Steel Research Laboratories
20-1, Shintomi, Futtsu, Chiba 293-8511

Manabu TAKAHASHI
Fellow, Ph.D.
General Manager, Sheet Products Lab.
Steel Research Laboratories

Nobuhiro FUJITA
Chief Researcher
Sheet Products Lab.
Steel Research Laboratories